Neurobiology of Aging 65 (2018) 121–131

Contents lists available at ScienceDirect

Neurobiology of Aging

journal homepage: www.elsevier.com/locate/neuaging

Joint associations of β-amyloidosis and cortical thickness with cognition

David S. Knopman [a,b,*], Emily S. Lundt [c], Terry M. Therneau [c], Prashanthi Vemuri [b,d], Val J. Lowe [b,d], Kejal Kantarci [b,d], Jeffrey L. Gunter [d,e], Matthew L. Senjem [d,e], Michelle M. Mielke [a,f], Mary M. Machulda [b,g], Rosebud O. Roberts [a,f], Bradley F. Boeve [a,b], David T. Jones [a,b,d], Ronald C. Petersen [a,b,f], Clifford R. Jack Jr [b,d]

[a] Department of Neurology, Mayo Clinic and Foundation, Rochester, MN, USA
[b] Mayo Clinic Alzheimer's Disease Research Center, Mayo Clinic and Foundation, Rochester, MN, USA
[c] Division of Biomedical Statistics and Informatics, Department of Health Sciences Research, Mayo Clinic and Foundation, Rochester, MN, USA
[d] Department of Radiology, Mayo Clinic and Foundation, Rochester, MN, USA
[e] Department of Information Technology, Mayo Clinic and Foundation, Rochester, MN, USA
[f] Division of Epidemiology, Department of Health Sciences Research, Mayo Clinic and Foundation, Rochester, MN, USA
[g] Division of Psychology, Department of Psychiatry, Mayo Clinic and Foundation, Rochester, MN, USA

ARTICLE INFO

Article history:
Received 30 October 2017
Received in revised form 12 January 2018
Accepted 22 January 2018
Available online 2 February 2018

Keywords:
Amyloid imaging
Neurodegeneration biomarkers
Structural MR imaging
Cognitive aging
Alzheimer's disease

ABSTRACT

In 1164 cognitively unimpaired persons, aged 50–95 years, from the population-based Mayo Clinic Study of Aging, we examined the relationships of baseline cognition and cognitive changes across the full range of cortical thickness of an Alzheimer signature region of interest and global β-amyloid levels measured by Pittsburgh compound B positron emission tomography (PIB PET) standardized uptake value ratio (SUVR). In machine-learning models accounting for both biomarkers simultaneously, worsening biomarker values were additive and associated with lower baseline global cognition and greater subsequent decline in global cognition. Associations between Alzheimer's disease signature cortical thickness or PIB PET β-amyloid SUVR and baseline cognition were mainly linear. Lower Alzheimer's disease signature cortical thickness values across the entire range of thickness predicted future decline in global cognitive scores, demonstrating its close relationship to cognitive functioning. PIB PET β-amyloid SUVR also predicted cognitive decline across its full range, even when cortical thickness was accounted for. PIB PET β-amyloid's relationship to cognitive decline was nonlinear, more prominent at lower β-amyloid levels and less prominent at higher β-amyloid levels.

1. Introduction

Understanding the pathophysiology of Alzheimer's disease (AD) has been greatly facilitated by the development of biomarkers. Studies of the relationship between β-amyloid positron emission tomography (PET) tracer levels and cognition in clinically normal persons generally show a modest inverse relationship (Donohue et al., 2017; Farrell et al., 2017; Hedden et al., 2013; Insel et al., 2016; Petersen et al., 2015; Villemagne et al., 2011). Measures of AD-related neurodegenerative processes such as cortical volume, cortical thickness, or glucose metabolic rate are more consistently associated with cognition (Fjell et al., 2014; Jack et al., 2015; Sabuncu et al., 2011; Weston et al., 2016; Wirth et al., 2013a). Examining associations of cognition with β-amyloid PET imaging markers and neurodegenerative imaging biomarkers individually has allowed for exploration of the full range of each feature but fails to account for the important inter-relationships of the two. Apparent associations between one of the biomarkers could be largely driven by variance shared with the other biomarker (Becker et al., 2011). Because of the difficulty in manipulating 2 complex functions in a single model simultaneously, most approaches seeking to examine the role of cognition as a function of β-amyloid PET imaging markers and neurodegenerative imaging biomarkers have been performed by dichotomizing each as normal or abnormal (Chetelat et al., 2012; Mattsson et al., 2015; Mormino et al., 2014; Villeneuve et al., 2014; Wirth et al., 2013b). Although categorical approaches are more tractable, large portions of the distribution of each biomarker conditioned on the presence of the other are left unexplored.

* Corresponding author at: Department of Neurology, Mayo Clinic, Rochester, MN 55905 USA. Tel.: +1 507 266 4106; fax: +1 507 538 6012.
E-mail address: knopman@mayo.edu (D.S. Knopman).

0197-4580/$ – see front matter © 2018 Elsevier Inc. All rights reserved.
https://doi.org/10.1016/j.neurobiolaging.2018.01.017

Based on recent models of the relationship between β-amyloidosis and neurodegeneration (Bloom, 2014; Hyman, 2011; Jack et al., 2013a; Jagust, 2016; Musiek and Holtzman, 2015), we hypothesized that (1) there would be additivity of elevated β-amyloid and declining cortical thickness for predicting level of cognitive functioning and (2) cortical thickness would be a better predictor of future cognitive decline than would β-amyloid. There have been many studies that examined both β-amyloid biomarkers and markers of neurodegeneration in cognitively normal persons as well as those with mild cognitive impairment. Those studies have consistently found that those in whom both biomarkers were abnormal had lower cognition and a worse prognosis than those with either only one of those biomarkers abnormal or with neither biomarker abnormal (see [Jack et al., 2016] for a summary of published studies). Second, prior studies have suggested that neurodegenerative biomarker levels were more strongly associated with cognition than was β-amyloidosis (Becker et al., 2011; Chetelat et al., 2012; Mattsson et al., 2015; Mormino et al., 2014; Vemuri et al., 2017a; Villeneuve et al., 2014; Wirth et al., 2013b). Because no prior study, to our knowledge, examined the associations in a multidimensional manner, we wished to determine whether the joint relationships between β-amyloid and cortical thickness versus cognition were linear or nonlinear. In the present analyses, we applied a flexible machine-learning model to explore in a 3-dimensional (3-D) space, the joint relationship between the continuous distributions of PET-derived β-amyloid deposition, MR-derived cortical thickness (as an imaging proxy for neurodegeneration), and cognition among cognitively unimpaired middle-aged and elderly individuals drawn from a population-based study.

2. Methods

2.1. Participants

Cognitively unimpaired participants from the Mayo Clinic Study of Aging (MCSA) were included in this longitudinal study if they were aged 50 years or older, had cognitive testing, had magnetic resonance imaging (MRI) and Pittsburgh compound B (PIB) PET scans, and had returned for one or more follow-up cognitive evaluations. Baseline was defined as an MCSA participant's first visit with cognitive testing and imaging.

The participants were adjudicated by a consensus panel as being cognitively unimpaired using previously described procedures (Petersen, 2004; Petersen et al., 2010; Roberts et al., 2008, 2012, 2014). The consensus panel consisted of a physician who examined the participant and performed a brief mental status examination, a study coordinator who interviewed both the participant and a study partner, and a neuropsychologist.

The neuropsychological test battery consisted of 9 instruments (Roberts et al., 2008) that were grouped into 4 domains: memory (Logical Memory-II [delayed recall], Visual Reproduction-II [delayed recall] from the Wechsler Memory Scale—Revised (Wechsler, 1987), and Auditory Verbal Learning Test [Ivnik et al., 1992]); attention/executive functioning (Trail Making Test B [Reitan, 1958], Digit Symbol Substitution test from the Wechsler Adult Intelligence Scale—Revised [Wechsler, 1981]); language (Boston Naming Test [Kaplan et al., 1978], category fluency [Lucas et al., 1998]); and visuospatial (picture completion and block design from the Wechsler Adult Intelligence Scale—Revised). Cognitive test scores were converted to z-scores based on a reference cohort of clinically normal MCSA participants aged 50–89 years enrolled between 2004 and 2012 and weighted to the Olmsted County population. Individual test z-scores were averaged to create a z-score for each of the 4 cognitive domains, and a global z-score was derived from the average of the 4 domain z-scores. We chose to use the global z-score to present our findings for data reduction purposes and because it generally reflected the key domains relevant to AD, namely memory and attention/executive.

2.2. Imaging

We took advantage of our prior work in selecting a set of regions that optimally distinguished persons in the AD pathway from those not in the pathway. Because of the computational intensity of our approach, we chose to limit our investigations to a single set of regions of interest (ROIs)—albeit ones with demonstrated validity for the AD pathway—for each biomarker. That meant that we did not select the identical ROIs for the 2 biomarkers. This is an implicit acknowledgement that, while cortical thickness has anatomic specificity for cognitive functions relevant to AD, β-amyloidosis may reflect more of a marker of network dysfunction.

PIB PET imaging used methods previously described (Jack et al., 2017). A PIB PET scan consisted of four 5-minute dynamic frames acquired from 40 to 60 minutes after injection of ^{11}C-PIB. The PIB PET ROIs were derived from an MRI template generated from each participant based on an in-house modification of the automated anatomic labeling atlas (Tzourio-Mazoyer et al., 2002). Regional PIB uptake was defined as the median uptake across all voxels in an ROI. A global PIB standardized uptake value ratio (SUVR) was calculated from a group of target regions in both hemispheres including parietal, cingulate precuneus, prefrontal, orbitofrontal, temporal, anterior cingulate, and posterior cingulate regions, with cerebellar crus serving as the reference region. This meta-ROI was based on our prior work (Jack et al., 2008) and has been validated neuropathologically (Murray et al., 2015). Target and reference regions were gray matter and white matter sharpened, and partial volume correction was not used. The global PIB meta-ROI SUVR is denoted as PIB PET SUVR in regions associated with β-amyloid (PIB_{AD}).

Cortical thickness measurements have several attractive methodological features that have led us to prefer it over gray matter regional density (e.g., Vemuri et al., 2009). Thickness can be measured reliably with widely available software (Schwarz et al., 2016b), and it is not sensitive to head size (Jack et al., 2015). Cortical thickness was measured as previously described (Jack et al., 2017). Cortical thickness in an AD signature meta-ROI represented an area-weighted average of mean cortical thickness across both hemispheres generated from the following FreeSurfer (v5.3) (http://surfer.nmr.mgh.harvard.edu) ROIs: entorhinal, inferior temporal, middle temporal, and fusiform. These regions were previously selected on the basis of discrimination between AD dementia and clinically normal individuals (Schwarz et al., 2016b; Whitwell et al., 2013). The AD signature meta-ROI cortical thickness is referred to as cortical thickness measured in an AD signature meta-ROI (TK_{AD}).

2.3. Statistical analyses

Cognition was modeled as a function of current age, PIB_{AD}, and TK_{AD} using a gradient boosting machines (GBMs) model, also adjusting for gender, education, and the number of exposures to the cognitive test battery before baseline. The number of cognitive test exposures before the study baseline is relevant because of learning effects in unimpaired individuals (Machulda et al., 2013). GBM is a machine-learning technique, which allows for arbitrary nonlinear and interaction effects that were particularly important in the 3-D space we were modeling. GBM fits a very large number of binary classification trees and then averages the results. The approach makes no assumptions about the functional form of the relationships. A strength of this particular method is avoidance of

overfitting (Friedman, 2001). For these models, we specified a monotonic relationship on age (increasing), PIB_{AD} (increasing), and TK_{AD} (decreasing), based on the expectation that their relationship with cognition should plateau or worsen but not improve. Because some participants had undergone cognitive testing before the first PIB PET, we also accounted for the number of prior exposures to cognitive testing and specified the monotonicity as improving to reflect the expectation of a learning effect. The GBM models allowed for an interaction depth of 2. The model complexity (number of subtrees) was chosen using 8-fold cross-validation. GBM package version 2.2 was used with the R statistical software version 3.3.1 (R Core Team [2016], R Foundation for Statistical Computing, Vienna).

We created 2 GBM models. From the first GBM model on predicted "baseline" cognition, global z-score (COG_b), we obtained model-based predictions in relation to TK_{AD} and PIB_{AD}. The second GBM model used annual change in global z-score (ΔCOG) predictions made in relation to TK_{AD} and PIB_{AD}. To develop a metric for ΔCOG, we derived slopes for each participant based on their serial cognitive testing using a linear mixed model adjusting for age, education, prior cognitive testing, and gender with random subject-specific intercepts and slopes. A natural cubic spline on age and education allowed us to capture potential nonlinearities. By fitting the model on the timescale, we can consider the slopes as an estimate of annualized cognitive change. To decrease the noise in the slope measurements, we included up to 2 cognitive testing values that preceded the PIB PET scan to be used in the calculation of slope.

We predicted the marginal effects of the selected variables (PIB_{AD}, TK_{AD}, and age) over the other covariates of gender, education, and prior exposure to cognitive testing. The output of the GBM model was visualized as a 3-D surface in which PIB_{AD} and TK_{AD} are represented on the x- and y-axes while predicted COG_b or ΔCOG is represented on the z-axis. MATLAB 2013a was used to generate the 3-D surface plots from the models (The MathWorks, Inc., Natick, MA, USA). Because there were age effects, we found it useful to present different age strata as individual plots. To make it easier to recognize contour lines and to apply tests of reliable differences, we also generated 2-D plots from the GBM model in which one imaging feature is represented on the x-axis and select values of the other imaging feature are depicted as a series of cubic smoothing spline curves representing fixed values of the other imaging feature.

Confidence limits for the contour plots and for the average difference between sets of lines were calculated using a bootstrap estimate. For each of 1000 bootstrap samples, a random set of subjects was chosen, with replacement, and a new GBM model was fitted to the resulting data set, the subsequent curves were derived, and results were tabulated over the 1000 resamples.

Statistical tests were presented for descriptive purposes; none of the sets of statistical tests were therefore corrected for multiple testing.

3. Results

Table 1 shows the demographic and imaging features of the 1164 participants, all of whom were cognitively unimpaired by a consensus diagnostic process. By virtue of the stratified sampling design of the MCSA, the group represented the 4 decades from ages 50 to 90 years approximately equally, with balance between men and women. In the analyses of the relationships between cognition and biomarkers to follow, differences between women and men were limited to a simple shift in COG_b (higher in women), so that all analyses are presented with men and women combined.

The distribution of COG_b and the ΔCOG is shown in Fig. 1, by age groups. Within the substantial variability of the relationship between COG_b and ΔCOG, lower baseline scores were more likely to be associated with more annual decline. With advancing age, COG_b was generally lower and ΔCOG larger.

Table 1
Demographic and imaging characteristics of MCSA participants who were cognitively unimpaired at baseline

Feature	Result
No. of participants	1164[a]
Age, y	
Mean (SD)	70 (10)
Median (IQR)	71 (63–77)
Range	51–95
Gender, male, no. (%)	611 (52%)
APOE ε4 carrier, no. (%)	316 (28%)
Education, y	
Mean (SD)	15 (3)
Number (%) of participants by number of exposures to cognitive testing before baseline imaging visit	
0	605 (52%)
1	255 (22%)
2+	304 (26%)
Global PIB SUVR	
Mean (SD)	1.5 (0.3)
Median (IQR)	1.3 (1.3, 1.5)
Range	1.0–3.2
AD signature thickness	
Mean (SD)	2.7 (0.1)
Median (IQR)	2.7 (2.6–2.8)
Range	2.2–3.1
Time in study, y	
Mean (SD)	3.1 (1.7)
Median (IQR)	2.6 (1.4, 4.3)
Range	1.0–7.1
Baseline MRI scan date range	Feb 2005 to Nov 2014
Baseline PIB PET scan date range	Jan 2006 to Nov 2014
Last follow-up date range	Oct 2007 to Feb 2016

Key: AD, Alzheimer's disease; IQR, interquartile range; MCSA, Mayo Clinic Study of Aging; PET, positron emission tomography; PIB, Pittsburgh compound B; SD, standard deviation; SUVR, standardized uptake value ratio.
[a] One thousand two hundred participants imaged of whom 36 lacked a usable baseline global z-score.

Fig. 2 shows the distributions of baseline TK_{AD} and PIB_{AD}. The PIB_{AD} distribution was highly skewed, which is evident even in the logarithmic scale in Fig. 2; the median value was 1.3 SUVR. TK_{AD} was more symmetrically distributed with a median of 2.7 mm. There was a strong age dependence of more abnormal values of TK_{AD} and PIB_{AD}. In the youngest decade of this population-based cohort, there were very few participants with $TK_{AD} < 2.67$ mm or $PIB_{AD} > 1.4$ (cut points previously derived in our laboratory [Jack et al., 2017]) and no one with both. However, in the older 3 groups, the number of participants with abnormal values (i.e., above the PIB_{AD} cut point and below the TK_{AD} cut point) increased substantially. Those with higher PIB_{AD} were likely to have lower TK_{AD}. Correlations between PIB_{AD} and TK_{AD} were age dependent: ages 50–59, rho = 0.05 (ns); 60–69, rho = −0.17 ($p = 0.002$); 70–79, rho = −0.13 ($p = 0.008$); and 80–89, rho = −0.10 ($p = 0.14$).

The relationship of PIB_{AD} and TK_{AD} to COG_b (Fig. 3) was represented as a surface that tilted downward in both x- and y-axes, reflecting the joint effect of both PIB_{AD} and TK_{AD} on cognition. There was a steepening of slope for COG_b at a TK_{AD} of approximately 2.5–2.6 mm. The bootstrap estimates of reliability showed that COG_b values were reliably worse at TK_{AD} of 2.3 or 2.5 mm than at thicker TK_{AD} values (Table 2). COG_b appeared linearly and inversely related to rising levels of PIB_{AD}. COG_b values at PIB_{AD} SUVR of 1.2 or 1.8 differed reliably only from those at the highest PIB_{AD} value; there was no difference in COG_b at the highest levels (2.1 vs. 2.5) of PIB_{AD}. The 2-D relationships are summarized in Fig. 4 across all ages and broken down by age decades in Supplemental Fig. 1.

The relationship of PIB_{AD} and TK_{AD} to ΔCOG also showed that both biomarkers contributed to predicting decline in cognition

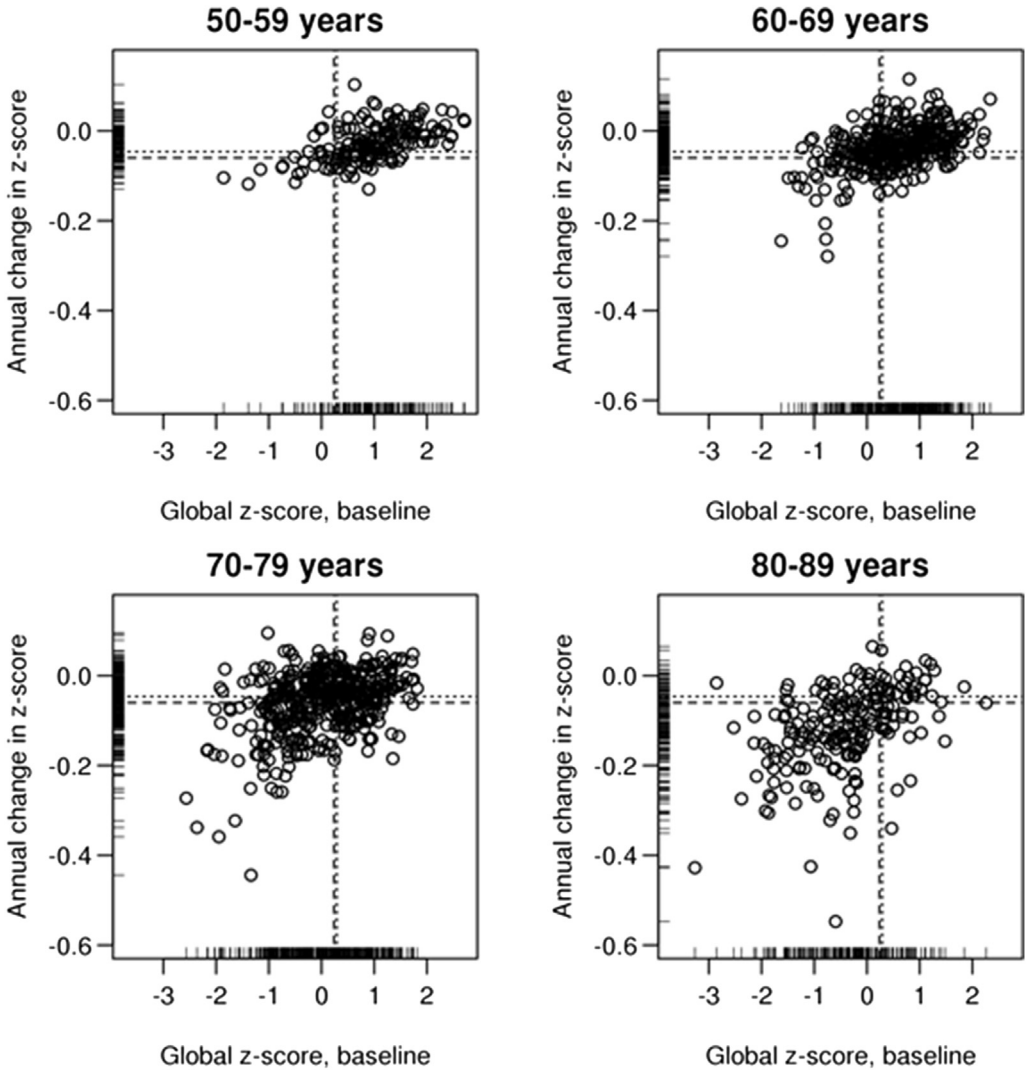

Fig. 1. The distribution of baseline global cognitive z-scores (x-axis) and the annualized change in global cognitive z-scores (y-axis) is shown by age groups: 50–59, 60–69, 70–79, and 80–89 years. For purposes of visual display, the change values were calculated from a linear mixed-effects model. We modeled log(global z-score) to estimate change expressed as a percentage per year. The overall mean (dashed lines) and median (dotted lines) values are indicated.

(Fig. 5). At more abnormal biomarker values, ΔCOG became larger (i.e., there was greater decline in cognition). The bootstrap estimates of reliability (Table 3) showed that ΔCOG declined monotonically from the highest TK_{AD} value to the lowest. PIB_{AD} also predicted ΔCOG across the full range of PIB_{AD}, but the reliability statistics showed that at $PIB_{AD} \geq 1.8$ SUVR, more abnormal values of PIB_{AD} were associated with a deceleration of ΔCOG. The 2-D relationships are summarized in Fig. 6 across all ages and broken down by age decades in Supplemental Fig. 2.

The GBM model for COG_b generated a table of the relative contributions of variables. In the model used for prediction of baseline cognition and including age, education, cognitive test cycle (overall number of cognitive test exposures), gender, APOE e4 genotype, TK_{AD}, and PIB_{AD}, age accounted for 40% of effects on cognition, education 23%, TK_{AD} 17%, and PIB_{AD} 14%. Sex was associated with only 3%, APOE e4 carriage 0.5%, and cognitive test cycle 1% of effects on cognition.

4. Discussion

Using a 3-D model in a population-based sample of cognitively unimpaired individuals aged 50–90 years, we found that cortical thickness (of a group of regions most affected in AD) and global measure of brain β-amyloid (as measured by PIB PET) were both related to baseline cognition and changes in cognition. We confirmed our first hypothesis that TK_{AD} and PIB_{AD} were additive with respect to cognitive function. Although the relationship of TK_{AD} to ΔCOG was mainly linear, PIB_{AD} SUVR >1.8 values predicted smaller values for ΔCOG compared to lower PIB_{AD} values. The differing shapes of the $TK_{AD} \times$ ΔCOG and $PIB_{AD} \times$ ΔCOG functions suggest, in accordance with our second hypothesis, that TK_{AD} may represent a more mechanistically proximate marker of the pathophysiology of cognitive decline than abnormal PIB_{AD}. Nonetheless, β-amyloid levels in the range observed in most of our cognitively unimpaired individuals demonstrated a relationship with declining cognition, even when cortical thickness was accounted for. Our findings are consistent with a model of sporadic late-onset AD in which lower levels of β-amyloid accelerate the deleterious effect of other neurodegenerative processes, which eventually become autonomous of β-amyloid, and then go on to cause cognitive decline (Bloom, 2014; Hyman, 2011; Jack et al., 2013a; Jagust, 2016; Musiek and Holtzman, 2015).

Cortical thickness in an AD-meta-ROI (TK_{AD}) is a prototypical biomarker of neurodegeneration, based on evidence from

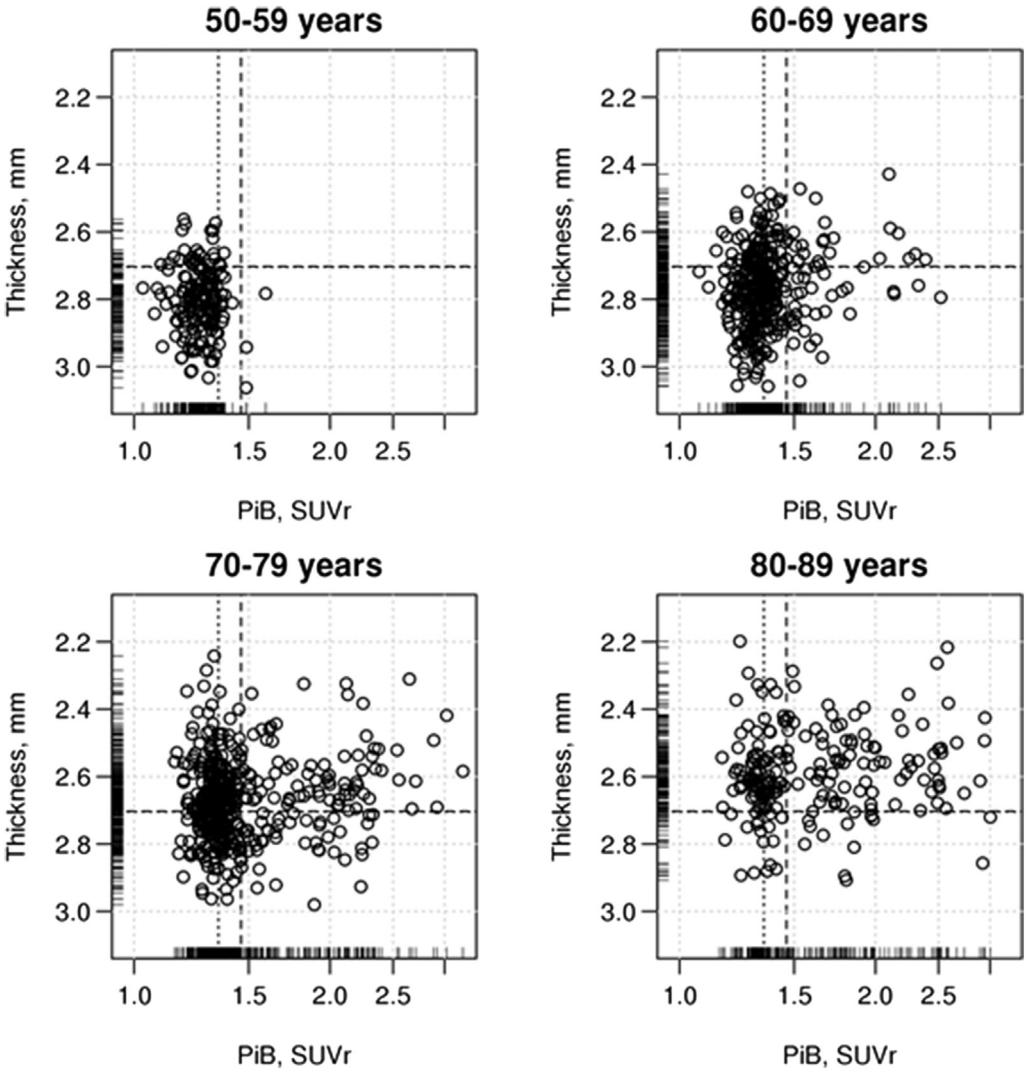

Fig. 2. The joint distribution of PIB_{AD} and TK_{AD} by decade of age. The scatterplot shows global β-amyloid in PIB SUVR units (PIB_{AD}) on the x-axis and AD signature cortical thickness (TK_{AD}) in millimeters at baseline on the y-axis, at baseline by decades of age: 50–59, 60–69, 70–79, and 80–89 years. PIB_{AD} is displayed on a logarithmic scale because of its highly skewed distribution. The overall mean (dashed lines) and median (dotted lines) values are indicated. Abbreviations: AD, Alzheimer's disease; PIB_{AD}, PIB PET SUVR in regions associated with β-amyloid; PIB PET, Pittsburgh compound B positron emission tomography; ROI, region of interest; SUVR, standardized uptake value ratio; TK_{AD}, cortical thickness measured in an AD signature meta-ROI.

antemortem clinical observations (Jack et al., 2015; Sabuncu et al., 2011; Weston et al., 2016; Wirth et al., 2013a); neuropathological observations (Giannakopoulos et al., 2003; Gomez-Isla et al., 1997; Savva et al., 2009); and prediction of future dementia (Bakkour et al., 2009, 2013; Dickerson and Wolk, 2012). Our current findings extend these prior studies by showing the quantitative relationships of cortical thickness to change in cognition in cognitively unimpaired people across the spectrum of β-amyloid levels. Visually (though not statistically), our modeling showed an increase in downward slope in ΔCOG at a TK_{AD} value around 2.6 mm, which corresponds to the cut point that we had derived using a different methodology (Jack et al., 2017). Both below and above that point, cognition was sensitive to TK_{AD}.

Despite its face validity, TK_{AD} is an incomplete biomarker for AD-related neurodegeneration. As shown elsewhere (Alexopoulos et al., 2014; Caroli et al., 2015; Jack et al., 2015; Toledo et al., 2014; Wirth et al., 2013a), cortical thickness has only moderate correlations with other measures of neurodegeneration, such as cerebrospinal fluid tau levels, hippocampal atrophy, or glucose metabolic rate by PET. Our findings are specific to cortical thickness in one meta-ROI and should not be mistaken as interchangeable with other biomarkers of neurodegeneration. Furthermore, loss of cortical thickness is not specific for AD, as other non-AD neurodegenerative (e.g., primary age-related tauopathy [Josephs et al., 2017] or vascular processes [e.g., overt cerebrovascular disease [Knopman et al., 2015b], metrics of cerebrovascular health [Leritz et al., 2011], or reduced cardiac output [Sabayan et al., 2015]) are associated with cortical thinning. Nonetheless, our findings demonstrate the linkage between declining cortical thickness in regions relevant to AD and cognition in cognitively unimpaired individuals.

The additive association of PIB_{AD} with TK_{AD} for cognition suggests that PIB_{AD} may be a proxy for neurodegenerative processes independent of cortical thickness. Elevated β-amyloidosis and neurodegeneration, broadly defined, are correlated (Dore et al., 2013; Fortea et al., 2014; Jack et al., 2013a; Villeneuve et al., 2014). It was this confound we sought to shed light on by evaluating PIB PET β-amyloid in the presence of cortical thickness. Indeed, PIB_{AD} in our GBM modeling was associated with cognition consistent with the observations in univariate analyses (Donohue et al., 2017; Hedden et al., 2013; Mormino et al., 2012; Petersen

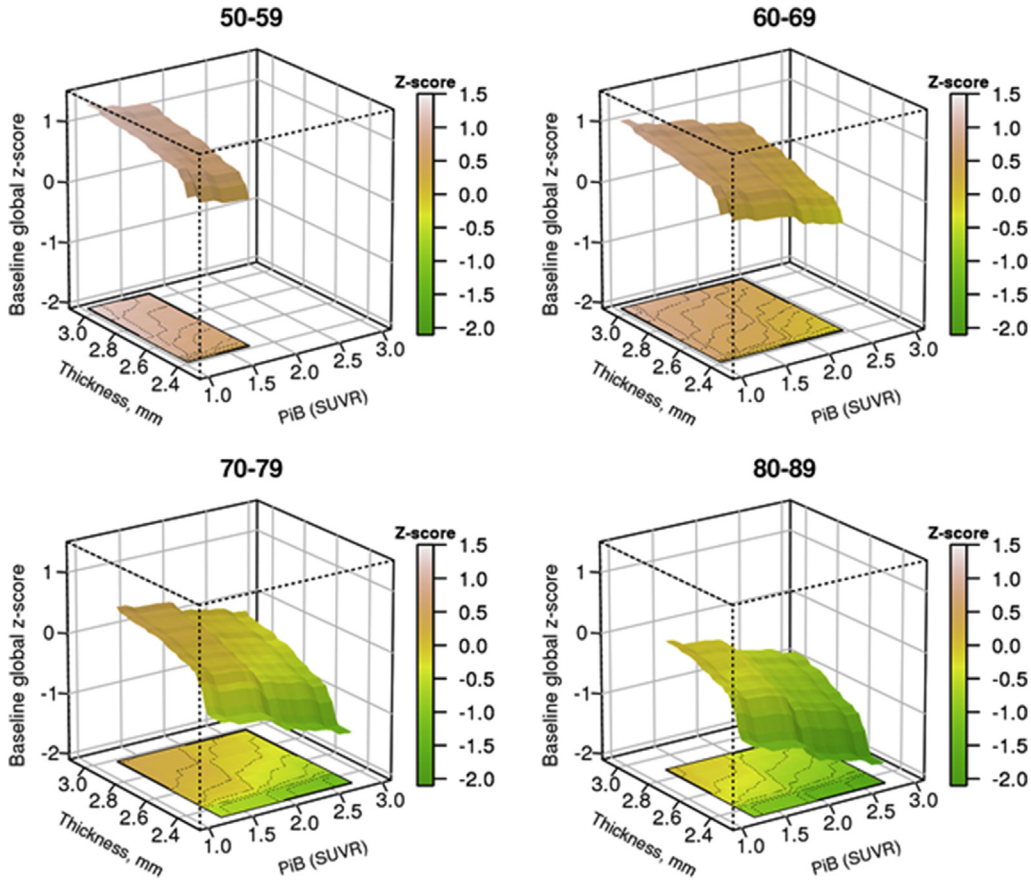

Fig. 3. Predicted average "baseline" cognitive global z-score (COG_b) from the GBM model by decade of age. Three-dimensional plot of PIB_{AD} (x-axis), TK_{AD} (y-axis), and COG_b (z-axis) for participants in the age ranges of 50–59, 60–69, 70–79, and 80–89 years. The color code to the right side of each figure depicts the level of COG_b. The surfaces are truncated according to the range of PIB_{AD} and TK_{AD} values that were found in each decade as shown in Fig. 2. Abbreviations: AD, Alzheimer's disease; GBM, gradient boosting machine; PIB_{AD}, PIB PET SUVR in regions associated with β-amyloid; PIB PET, Pittsburgh compound B positron emission tomography; ROI, region of interest; SUVR, standardized uptake value ratio; TK_{AD}, cortical thickness measured in an AD signature meta-ROI. (For interpretation of the references to color in this figure legend, the reader is referred to the Web version of this article.)

et al., 2015; Villeneuve et al., 2015). Others have also asserted that the relationship of cortical β-amyloidosis to cognition is through neurodegeneration (Becker et al., 2011; Chetelat et al., 2012; Mattsson et al., 2015; Mormino et al., 2014; Villeneuve et al., 2014; Wirth et al., 2013b). Elevated β-amyloid levels, even in cognitively unimpaired persons, are associated with higher tau PET signal (Vemuri et al., 2017b).

Table 2
Differences in predicted cognition according to different levels of TK_{AD} and PIB_{AD}, from 1000 replications with replacement

Thickness	PIB	Mean (SD)	95% confidence interval	*p*-value
2.3 versus 2.5	Fixed	−0.579 (0.144)	−0.86, −0.30	<0.001
2.3 versus 2.7	Fixed	−0.870 (0.173)	−1.21, −0.53	<0.001
2.3 versus 3	Fixed	−1.156 (0.201)	−1.55, −0.76	<0.001
2.5 versus 2.7	Fixed	−0.291 (0.102)	−0.49, −0.09	0.004
2.5 versus 3	Fixed	−0.576 (0.151)	−0.87, −0.28	<0.001
2.7 versus 3	Fixed	−0.285 (0.113)	−0.51, −0.06	0.01
Fixed	1.2 versus 1.8	0.228 (0.084)	0.06, 0.39	0.007
Fixed	1.2 versus 2.1	0.423 (0.135)	0.16, 0.69	0.002
Fixed	1.2 versus 2.5	0.629 (0.159)	0.32, 0.94	<0.001
Fixed	1.8 versus 2.1	0.195 (0.099)	0.00, 0.39	0.05
Fixed	1.8 versus 2.5	0.401 (0.129)	0.15, 0.65	0.002
Fixed	2.1 versus 2.5	0.206 (0.104)	0.00, 0.41	0.05

Values across age groups are averaged.
Key: AD, Alzheimer's disease; PIB_{AD}, PIB PET SUVR in regions associated with β-amyloid; PIB PET, Pittsburgh compound B positron emission tomography; ROI, region of interest; SD, standard deviation; SUVR, standardized uptake value ratio; TK_{AD}, cortical thickness measured in an AD signature meta-ROI.

Our results showed a diminution of the association of cognitive decline with PIB_{AD} SUVR >1.8, suggesting that higher PIB_{AD} levels are less strongly linked to neurodegeneration. We cannot exclude the possibility that associations between β-amyloidosis at high PIB_{AD} levels and cognition could be mediated by some other β-amyloid species not detected by PIB PET (e.g., oligomers [Esparza et al., 2013]). However, the dramatically long time period and slow rate over which β-amyloid accumulation occurs preclinically (Jack et al., 2013b; Rowe et al., 2010; Villemagne et al., 2013) could contribute to the delinking of high levels of β-amyloid and subsequent cognitive decline. It is likely that β-amyloid levels are an indicator of the maturity of neuronal dysfunction induced by non–β-amyloid mechanisms.

Age had large effects on baseline cognition and on biomarker levels. As shown in Fig. 1, very few study participants aged less than 60 years experienced cognitive decline. Fig. 2 shows the increasing proportion of participants over age 70 years with TK_{AD} <2.5 mm, in keeping with well-recognized declines in cortical thickness that occur with aging (Fjell et al., 2014; Knopman et al., 2016; Raz et al., 2005; Salat et al., 2004). Age has a similarly substantial role in driving associations with cortical thickness in persons with AD dementia (Knopman et al., 2016). The same was true for the strong age dependence of elevated brain β-amyloid (Jack et al., 2014). The other confounding effect of age is that cerebrovascular disease and

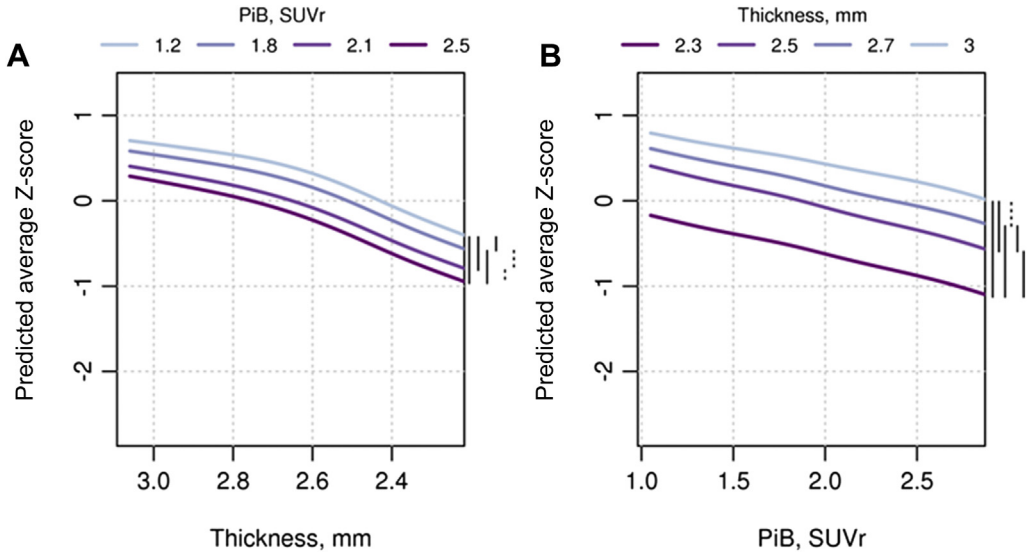

Fig. 4. Two-dimensional renderings show (A) TK_{AD} (y-axis) by COG_b (z-axis) with 4 levels of PIB_{AD}: PIB SUVR values of 1.2, 1.8, 2.1, and 2.5 and (B) PIB_{AD} (x-axis) by COG_b (z-axis) with 4 levels of TK_{AD}: cortical thickness in mm: 3, 2.7, 2.5, and 2.3. The curves are combined across ages, and on the right hand side of each figure, a bar coding scheme summarizes the reliability statistics (see Table 2 for means and confidence intervals of pairwise differences). The 2-D renderings for each age group are shown in Supplemental Fig. 1. Solid lines $p < 0.01$; dashed lines $0.01<p<0.05$; gray dashed $p > 0.05$. Abbreviations: AD, Alzheimer's disease; COG_b, predicted "baseline" cognition, global z-score; PIB_{AD}, PIB PET SUVR in regions associated with β-amyloid; PIB PET, Pittsburgh compound B positron emission tomography; ROI, region of interest; SUVR, standardized uptake value ratio; TK_{AD}, cortical thickness measured in an AD signature meta-ROI.

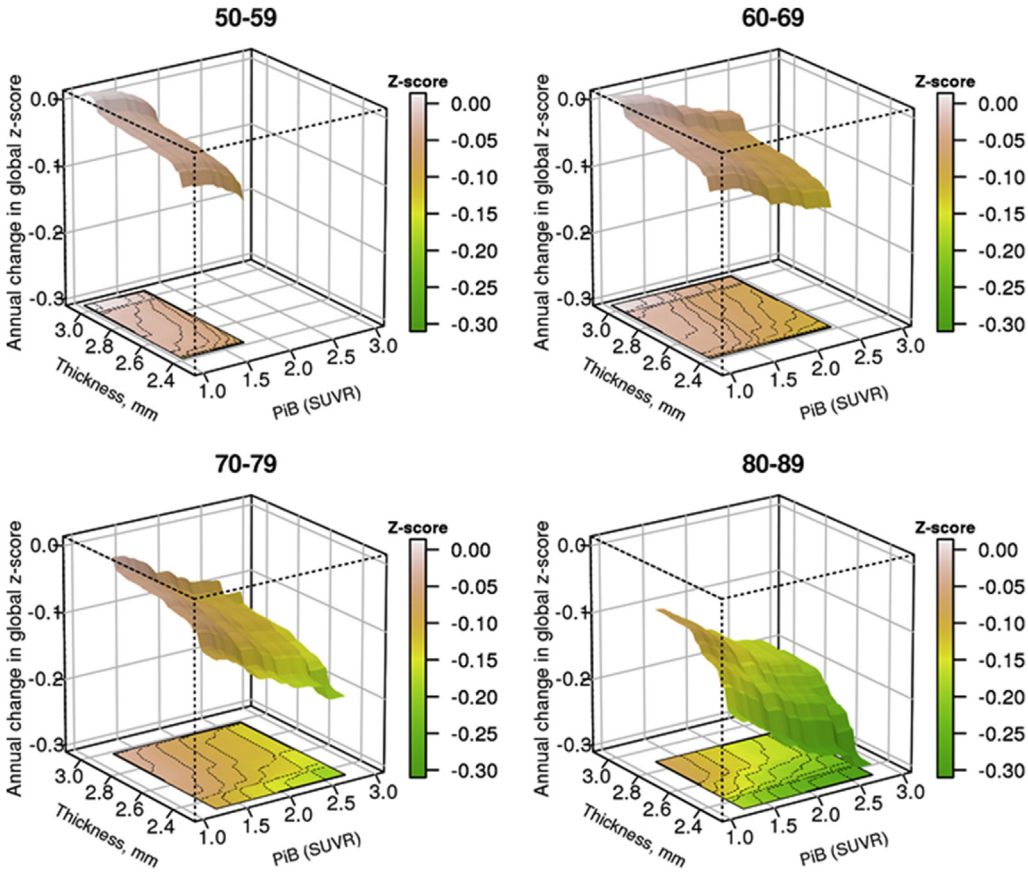

Fig. 5. Predicted average annual change in cognitive global z-score (ΔCOG) from the GBM model by decade of age. ΔCOG is a slope estimate calculated for each participant based on their serial cognitive testing using linear mixed models to represent annualized cognitive change. Three-dimensional plot of PIB_{AD} (x-axis), TK_{AD} (y-axis), and ΔCOG (z-axis) for participants in the age ranges of 50–59, 60–69, 70–79, and 80–89 years. The color code to the right side of each figure quantitates ΔCOG. The surfaces are truncated according to the range of PIB_{AD} and TK_{AD} values that were found in each decade as shown in Fig. 2. Abbreviations: AD, Alzheimer's disease; GBM, gradient boosting machine; PIB_{AD}, PIB PET SUVR in regions associated with β-amyloid; PIB PET, Pittsburgh compound B positron emission tomography; ROI, region of interest; SUVR, standardized uptake value ratio; TK_{AD}, cortical thickness measured in an AD signature meta-ROI. (For interpretation of the references to color in this figure legend, the reader is referred to the Web version of this article.)

Table 3
Differences in estimates of change in cognition according to different levels of TK_{AD} and PIB_{AD}, from 1000 replications with replacement

Thickness	PIB	Mean (SD)	95% confidence interval	*p*-value
2.3 versus 2.5	Fixed	−0.037 (0.019)	−0.07, 0.00	0.06
2.3 versus 2.7	Fixed	−0.056 (0.026)	−0.11, −0.01	0.03
2.3 versus 3	Fixed	−0.074 (0.027)	−0.13, −0.02	0.005
2.5 versus 2.7	Fixed	−0.020 (0.013)	−0.05, 0.01	0.14
2.5 versus 3	Fixed	−0.038 (0.015)	−0.07, −0.01	0.01
2.7 versus 3	Fixed	−0.018 (0.007)	(−0.03, −0.00)	0.009
Fixed	1.2 versus 1.8	0.036 (0.013)	0.01, 0.06	0.006
Fixed	1.2 versus 2.1	0.050 (0.016)	0.02, 0.08	0.002
Fixed	1.2 versus 2.5	0.066 (0.018)	0.03, 0.10	<0.001
Fixed	1.8 versus 2.1	0.014 (0.009)	−0.00, 0.03	0.13
Fixed	1.8 versus 2.5	0.030 (0.013)	0.00, 0.06	0.03
Fixed	2.1 versus 2.5	0.017 (0.012)	−0.01, 0.04	0.15

Key: AD, Alzheimer's disease; PIB_{AD}, PIB PET SUVR in regions associated with β-amyloid; PIB PET, Pittsburgh compound B positron emission tomography; ROI, region of interest; SD, standard deviation; SUVR, standardized uptake value ratio; TK_{AD}, cortical thickness measured in an AD signature meta-ROI.

non-AD neurodegenerative diseases increase in prevalence with advancing age (Nelson et al., 2011); their presence could attenuate associations between cognition and β-amyloidosis or cortical thickness. Despite all these age-dependent differences, the GBM model showed that the joint relationships between cortical thickness and brain β-amyloid to cognition were very similar across ages 50 and 90 years.

Our results show the limitations of using dichotomous models to characterize cortical thickness and brain β-amyloid: within the "normal" and "abnormal" ranges of each biomarker, cognition varies over a substantial range. On the other hand, the modest amount of nonlinearity plus the clear demonstration of the additive effects of PIB_{AD} and TK_{AD} support the use of dichotomous models.

Strengths of our analysis included the large, well-characterized cohort and the ability to implement the GBM model. In contrast to linear mixed models, GBM has a number of advantages, the 2 major ones being that GBM makes no assumptions about the functional form of relationship and that GBM does not result in overfitting of the data. Its disadvantage is that as currently operationalized, the method requires a bootstrap method to generate measures of statistical reliability.

There were limitations to our analyses that were necessitated by our strategic focus on cognitively unimpaired individuals and limitations imposed by the complexity of the processes we studied. Thus, there was a truncated range of cortical thickness, β-amyloid, and cognitive function because our analyses included only unimpaired individuals. Second, we included individuals who were given consensus diagnoses of cognitively unimpaired. We strongly favor the use of consensus clinical diagnoses based on discussion among the clinicians who interacted with the participant because expert consensus diagnoses are an efficient way to include information from different sources into a single diagnosis. That meant that a small fraction of persons (4.5%) in our study group had global z-scores that were worse than −1.5, the commonly used but arbitrary cut score for cognitive impairment (Knopman et al., 2015a). We reran our analyses excluding these individuals, and there were no differences in outcomes. We therefore retained these individuals in our analyses to maintain consistency with our prior and future publications. Third, we focused on global cognition rather than individual domains to demonstrate relationships. We have conducted analyses with memory or attention/executive cognitive domains and found very similar relationships to those with global cognition. Furthermore, the current cortical thickness meta-ROI is the one our laboratory is using in categorical analyses. Fourth, our period of follow-up was relatively short. While that attenuated effects of drop-out, short observation periods make determinations of cognitive changes in high-functioning persons noisy. We attempted to mitigate that problem by including cognitive test data from visits that preceded the initial imaging visit. Fifth, we chose to examine only one cortical thickness meta-ROI rather than to perform the analyses either on all ROI's or on all cortical voxels. Prior analyses demonstrated that the AD signature ROI that we used faithfully

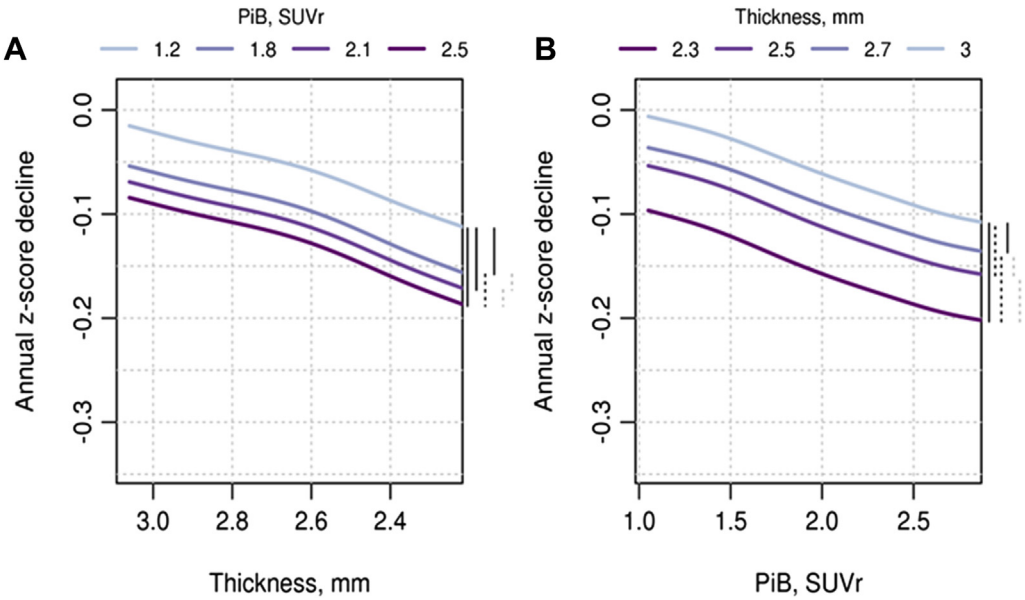

Fig. 6. Two-dimensional renderings show (A) TK_{AD} (y-axis) by ΔCOG (z-axis) with 4 levels of PIB_{AD}: PIB SUVR values of 1.2, 1.8, 2.1, and 2.5 and (B) PIB_{AD} (x-axis) by ΔCOG (z-axis) with 4 levels of TK_{AD}: cortical thickness in mm: 3, 2.7, 2.5, and 2.3. The curves are combined across ages and on the right hand side of each figure, a bar coding scheme shows the reliability statistics (see Table 3 for means and confidence intervals of pairwise differences). The 2-D renderings for each age group are shown in Supplemental Fig. 1. Solid lines $p < 0.01$; dashed lines $0.01 < p < 0.05$; gray dashed $p > 0.05$. Abbreviations: AD, Alzheimer's disease; ΔCOG, annual change in global z-score; PIB_{AD}, PIB PET SUVR in regions associated with β-amyloid; PIB PET, Pittsburgh compound B positron emission tomography; ROI, region of interest; SUVR, standardized uptake value ratio; TK_{AD}, cortical thickness measured in an AD signature meta-ROI.

reflected volumetric changes in persons in the AD pathway (Schwarz et al., 2016b; Whitwell et al., 2013).

Finally, we did not include tau PET in our analyses. Although regional tau PET and cortical thickness are strongly correlated in persons with AD dementia (Xia et al., 2017), the low tau PET signal outside the medial temporal lobe in cognitively unimpaired individuals (Brier et al., 2016; Cho et al., 2016; Johnson et al., 2015; Ossenkoppele et al., 2016; Scholl et al., 2016; Schwarz et al., 2016a) will present unique challenges to modeling that are beyond the scope of the current analyses.

Disclosure statement

Dr. Knopman serves on a Data Safety Monitoring Board for the DIAN study and previously had served on a Data Safety Monitoring Board for Lundbeck Pharmaceuticals; is an investigator in clinical trials sponsored by Biogen, Lilly Pharmaceuticals, and the AD Cooperative Study; and receives research support from the NIH. Dr. Jack serves on scientific advisory board for Eli Lilly & Company; receives research support from the NIH/NIA, and the Alexander Family AD Research Professorship of the Mayo Foundation; and holds stock in Johnson & Johnson. Ms. Lundt reports no disclosures. Dr. Vemuri receives research grants from the NIH/NIA. Dr. Mielke served as a consultant to Eli Lilly and Lysosomal Therapeutics, Inc. She receives research support from the National Institutes of Health (R01 AG49704, P50 AG44170, U01 AG06786, RF1 AG55151); Department of Defense (W81XWH-15-1); and unrestricted research grants from Biogen, Roche, and Lundbeck. Dr. Machulda receives research support from the NIH/NIA and NIDCD. Dr. Lowe serves on scientific advisory boards for Bayer Schering Pharma, Merck Research, Piramal Life Sciences and receives research support from GE Healthcare, Siemens Molecular Imaging, AVID Radiopharmaceuticals, and the NIH (NIA, NCI). Dr. Kantarci receives research grants from the NIH/NIA. Dr. Gunter reports no disclosures. Mr. Senjem reports no disclosures. Dr. Jones reports no disclosures. Dr. Roberts reports no disclosures. She receives research grants from the NIH/NIA. Dr. Boeve has served as an investigator for clinical trials sponsored by GE Healthcare, FORUM Pharmaceuticals, C2N Diagnostics, and Axovant. He receives publishing royalties from Behavioral Neurology of Dementia (Cambridge Medicine, 2009, 2016). He serves on the Scientific Advisory Board of the Tau Consortium. He receives research support from the NIH, the Mayo Clinic Dorothy, Harry T. Mangurian Jr. Lewy Body Dementia Program, and the Little Family Foundation. Dr. Therneau receives research grants from the NIH. Dr. Petersen serves on data monitoring committees for Janssen Alzheimer Immunotherapy and is a consultant for Biogen, Roche, Merck, Genentech, Inc; receives publishing royalties from Mild Cognitive Impairment (Oxford University Press, 2003); and receives research support from the NIH/NIA.

Acknowledgements

Authors' contributions: DSK generated first draft and completed final draft and contributed to study concept and design, acquisition of data, analysis and interpretation, critical revision of the article for important intellectual content. CRJ helped in analysis and interpretation, critical revision of the article for important intellectual content, and study supervision. ESL helped in analysis and interpretation, and critical revision of the article for important intellectual content. PV, Michelle MM, Mary MM, VJL, KK, JLG, DTJ, and ROR contributed to critical revision of the article for important intellectual content. MLS helped in analysis, critical revision of the article for important intellectual content. BFB contributed to acquisition of data, and critical revision of the article for important intellectual content. TMT devised analytic plan and helped in analysis and interpretation, critical revision of the article for important intellectual content, and study supervision. RCP contributed to acquisition of data, critical revision of the article for important intellectual content, and study supervision. Statistical analysis was performed by EL and TT.

This work was supported by NIH grants P50 AG16574, U01 AG06786, R01 AG034676, R01 AG41851, and R01 AG11378; the Elsie and Marvin Dekelboum Family Foundation; the Robert H. and Clarice Smith and Abigail Van Buren AD Research Program of the Mayo Foundation; GHR Foundation; Alexander Family AD Research Professorship of the Mayo Clinic; a Liston Award; Schuler Foundation; and the Mayo Foundation for Medical Education and Research.

Appendix A. Supplementary data

Supplementary data associated with this article can be found, in the online version, at https://doi.org/10.1016/j.neurobiolaging.2018.01.017.

References

Alexopoulos, P., Kriett, L., Haller, B., Klupp, E., Gray, K., Grimmer, T., Laskaris, N., Forster, S., Perneczky, R., Kurz, A., Drzezga, A., Fellgiebel, A., Yakushev, I., 2014. Limited agreement between biomarkers of neuronal injury at different stages of Alzheimer's disease. Alzheimers Dement. 10, 684–689.

Bakkour, A., Morris, J.C., Dickerson, B.C., 2009. The cortical signature of prodromal AD: regional thinning predicts mild AD dementia. Neurology 72, 1048–1055.

Bakkour, A., Morris, J.C., Wolk, D.A., Dickerson, B.C., 2013. The effects of aging and Alzheimer's disease on cerebral cortical anatomy: specificity and differential relationships with cognition. Neuroimage 76, 332–344.

Becker, J.A., Hedden, T., Carmasin, J., Maye, J., Rentz, D.M., Putcha, D., Fischl, B., Greve, D.N., Marshall, G.A., Salloway, S., Marks, D., Buckner, R.L., Sperling, R.A., Johnson, K.A., 2011. Amyloid-beta associated cortical thinning in clinically normal elderly. Ann. Neurol. 69, 1032–1042.

Bloom, G.S., 2014. Amyloid-beta and tau: the trigger and bullet in Alzheimer disease pathogenesis. JAMA Neurol. 71, 505–508.

Brier, M.R., Gordon, B., Friedrichsen, K., McCarthy, J., Stern, A., Christensen, J., Owen, C., Aldea, P., Su, Y., Hassenstab, J., Cairns, N.J., Holtzman, D.M., Fagan, A.M., Morris, J.C., Benzinger, T.L., Ances, B.M., 2016. Tau and Abeta imaging, CSF measures, and cognition in Alzheimer's disease. Sci. Transl. Med. 8, 338ra366.

Caroli, A., Prestia, A., Galluzzi, S., Ferrari, C., van der Flier, W.M., Ossenkoppele, R., Van Berckel, B., Barkhof, F., Teunissen, C., Wall, A.E., Carter, S.F., Scholl, M., Choo, I.H., Grimmer, T., Redolfi, A., Nordberg, A., Scheltens, P., Drzezga, A., Frisoni, G.B., 2015. Mild cognitive impairment with suspected nonamyloid pathology (SNAP): prediction of progression. Neurology 84, 508–515.

Chetelat, G., Villemagne, V.L., Villain, N., Jones, G., Ellis, K.A., Ames, D., Martins, R.N., Masters, C.L., Rowe, C.C., 2012. Accelerated cortical atrophy in cognitively normal elderly with high beta-amyloid deposition. Neurology 78, 477–484.

Cho, H., Choi, J.Y., Hwang, M.S., Kim, Y.J., Lee, H.M., Lee, H.S., Lee, J.H., Ryu, Y.H., Lee, M.S., Lyoo, C.H., 2016. In vivo cortical spreading pattern of tau and amyloid in the Alzheimer disease spectrum. Ann. Neurol. 80, 247–258.

Dickerson, B.C., Wolk, D.A., 2012. MRI cortical thickness biomarker predicts AD-like CSF and cognitive decline in normal adults. Neurology 78, 84–90.

Donohue, M.C., Sperling, R.A., Petersen, R., Sun, C.K., Weiner, M.W., Aisen, P.S., 2017. Association between elevated brain amyloid and subsequent cognitive decline among cognitively normal persons. JAMA 317, 2305–2316.

Dore, V., Villemagne, V.L., Bourgeat, P., Fripp, J., Acosta, O., Chetelat, G., Zhou, L., Martins, R., Ellis, K.A., Masters, C.L., Ames, D., Salvado, O., Rowe, C.C., 2013. Cross-sectional and longitudinal analysis of the relationship between Abeta deposition, cortical thickness, and memory in cognitively unimpaired individuals and in Alzheimer disease. JAMA Neurol. 70, 903–911.

Esparza, T.J., Zhao, H., Cirrito, J.R., Cairns, N.J., Bateman, R.J., Holtzman, D.M., Brody, D.L., 2013. Amyloid-beta oligomerization in Alzheimer dementia versus high-pathology controls. Ann. Neurol. 73, 104–119.

Farrell, M.E., Kennedy, K.M., Rodrigue, K.M., Wig, G., Bischof, G.N., Rieck, J.R., Chen, X., Festini, S.B., Devous Sr., M.D., Park, D.C., 2017. Association of longitudinal cognitive decline with amyloid burden in middle-aged and older adults: evidence for a dose-response relationship. JAMA Neurol. 74, 830–838.

Fjell, A.M., Westlye, L.T., Grydeland, H., Amlien, I., Espeseth, T., Reinvang, I., Raz, N., Dale, A.M., Walhovd, K.B., 2014. Accelerating cortical thinning: unique to dementia or universal in aging? Cereb. Cortex 24, 919–934.

Fortea, J., Vilaplana, E., Alcolea, D., Carmona-Iragui, M., Sanchez-Saudinos, M.B., Sala, I., Anton-Aguirre, S., Gonzalez, S., Medrano, S., Pegueroles, J., Morenas, E., Clarimon, J., Blesa, R., Lleo, A., 2014. Cerebrospinal fluid beta-amyloid and phospho-tau biomarker interactions affecting brain structure in preclinical Alzheimer disease. Ann. Neurol. 76, 223–230.

Friedman, J., 2001. Greedy function approximation: a gradient boosting machine. Ann. Stat. 29, 1189–1232.
Giannakopoulos, P., Herrmann, F.R., Bussiere, T., Bouras, C., Kovari, E., Perl, D.P., Morrison, J.H., Gold, G., Hof, P.R., 2003. Tangle and neuron numbers, but not amyloid load, predict cognitive status in Alzheimer's disease. Neurology 60, 1495–1500.
Gomez-Isla, T., Hollister, R., West, H., Mui, S., Growdon, J.H., Petersen, R.C., Parisi, J.E., Hyman, B.T., 1997. Neuronal loss correlates with but exceeds neurofibrillary tangles in Alzheimer's disease. Ann. Neurol. 41, 17–24.
Hedden, T., Oh, H., Younger, A.P., Patel, T.A., 2013. Meta-analysis of amyloid-cognition relations in cognitively normal older adults. Neurology 80, 1341–1348.
Hyman, B.T., 2011. Amyloid-dependent and amyloid-independent stages of Alzheimer disease. Arch. Neurol. 68, 1062–1064.
Insel, P.S., Donohue, M.C., Mackin, R.S., Aisen, P.S., Hansson, O., Weiner, M.W., Mattsson, N., 2016. Cognitive and functional changes associated with Abeta pathology and the progression to mild cognitive impairment. Neurobiol. Aging 48, 172–181.
Ivnik, R.J., Malec, J.F., Smith, G.E., Tangalos, E., Petersen, R.C., Kokmen, E., Kurland, L.T., 1992. Mayo's older Americans normative studies updated AVLT norms for ages 59-97. Clin. Neuropsychol. 6 (suppl), 83–104.
Jack Jr., C.R., Knopman, D.S., Chetelat, G., Dickson, D., Fagan, A.M., Frisoni, G.B., Jagust, W., Mormino, E.C., Petersen, R.C., Sperling, R.A., van der Flier, W.M., Villemagne, V.L., Visser, P.J., Vos, S.J., 2016. Suspected non-Alzheimer disease pathophysiology - concept and controversy. Nat. Rev. Neurol. 12, 117–124.
Jack Jr., C.R., Knopman, D.S., Jagust, W.J., Petersen, R.C., Weiner, M.W., Aisen, P.S., Shaw, L.M., Vemuri, P., Wiste, H.J., Weigand, S.D., Lesnick, T.G., Pankratz, V.S., Donohue, M.C., Trojanowski, J.Q., 2013a. Tracking pathophysiological processes in Alzheimer's disease: an updated hypothetical model of dynamic biomarkers. Lancet Neurol. 12, 207–216.
Jack Jr., C.R., Lowe, V.J., Senjem, M.L., Weigand, S.D., Kemp, B.J., Shiung, M.M., Knopman, D.S., Boeve, B.F., Klunk, W.E., Mathis, C.A., Petersen, R.C., 2008. 11C PiB and structural MRI provide complementary information in imaging of Alzheimer's disease and amnestic mild cognitive impairment. Brain 131, 665–680.
Jack Jr., C.R., Wiste, H.J., Lesnick, T.G., Weigand, S.D., Knopman, D.S., Vemuri, P., Pankratz, V.S., Senjem, M.L., Gunter, J.L., Mielke, M.M., Lowe, V.J., Boeve, B.F., Petersen, R.C., 2013b. Brain beta-amyloid load approaches a plateau. Neurology 80, 890–896.
Jack Jr., C.R., Wiste, H.J., Weigand, S.D., Rocca, W.A., Knopman, D.S., Mielke, M.M., Lowe, V.J., Senjem, M.L., Gunter, J.L., Preboske, G.M., Pankratz, V.S., Vemuri, P., Petersen, R.C., 2014. Age-specific population frequencies of cerebral beta-amyloidosis and neurodegeneration among people with normal cognitive function aged 50-89 years: a cross-sectional study. Lancet Neurol. 13, 997–1005.
Jack, C.R., Wiste, H.J., Weigand, S.D., Therneau, T.M., Lowe, V.J., Knopman, D.S., Gunter, J.L., Senjem, M.L., Jones, D.T., Kantarci, K., Machulda, M.M., Mielke, M.M., Roberts, R.O., Vemuri, P., Reyes, D., Petersen, R.C., 2017. Defining imaging biomarker cut-points for brain aging and Alzheimer's disease. Alzheimer's Demen. 13, 205–216.
Jack, C.R.J., Wiste, H.J., Weigand, S.D., Knopman, D.S., Mielke, M.M., Vemuri, P., Lowe, V., Senjem, M.L., Gunter, J.L., Reyes, D., Machulda, M.M., Roberts, R., Petersen, R.C., 2015. Different definitions of neurodegeneration produce similar frequencies of amyloid and neurodegeneration biomarker groups by age among cognitively non-impaired individuals. Brain 138, 3747–3759.
Jagust, W., 2016. Is amyloid-beta harmful to the brain? Insights from human imaging studies. Brain 139, 23–30.
Johnson, K.A., Schultz, A., Betensky, R.A., Becker, J.A., Sepulcre, J., Rentz, D., Mormino, E., Chhatwal, J., Amariglio, R., Papp, K., Marshall, G., Albers, M., Mauro, S., Pepin, L., Alverio, J., Judge, K., Philiossaint, M., Shoup, T., Yokell, D., Dickerson, B., Gomez-Isla, T., Hyman, B., Vasdev, N., Sperling, R., 2015. Tau PET imaging in aging and early Alzheimer's disease. Ann. Neurol. 79, 110–119.
Josephs, K.A., Murray, M.E., Tosakulwong, N., Whitwell, J.L., Knopman, D.S., Machulda, M.M., Weigand, S.D., Boeve, B.F., Kantarci, K., Petrucelli, L., Lowe, V.J., Jack Jr., C.R., Petersen, R.C., Parisi, J.E., Dickson, D.W., 2017. Tau aggregation influences cognition and hippocampal atrophy in the absence of beta-amyloid: a clinico-imaging-pathological study of primary age-related tauopathy (PART). Acta Neuropathol. 133, 705–715.
Kaplan, E., Goodglass, H., Weintraub, S., 1978. The Boston Naming Test, second ed. Lea & Fabiger, Boston.
Knopman, D.S., Beiser, A., Machulda, M.M., Fields, J., Roberts, R.O., Pankratz, V.S., Aakre, J., Cha, R.H., Rocca, W.A., Mielke, M.M., Boeve, B.F., Devine, S., Ivnik, R.J., Au, R., Auerbach, S., Wolf, P.A., Seshadri, S., Petersen, R.C., 2015a. Spectrum of cognition short of dementia: Framingham Heart Study and Mayo Clinic Study of Aging. Neurology 85, 1712–1721.
Knopman, D.S., Griswold, M.E., Lirette, S.T., Gottesman, R.F., Kantarci, K., Sharrett, A.R., Jack Jr., C.R., Graff-Radford, J., Schneider, A.L., Windham, B.G., Coker, L.H., Albert, M.S., Mosley Jr., T.H., 2015b. Vascular imaging abnormalities and cognition: mediation by cortical volume in nondemented individuals: atherosclerosis risk in communities-neurocognitive study. Stroke 46, 433–440.
Knopman, D.S., Jack Jr., C.R., Wiste, H.J., Weigand, S.D., Vemuri, P., Lowe, V.J., Kantarci, K., Gunter, J.L., Senjem, M.L., Mielke, M.M., Machulda, M.M., Roberts, R.O., Boeve, B.F., Jones, D.T., Petersen, R.C., 2016. Age and neurodegeneration imaging biomarkers in persons with Alzheimer disease dementia. Neurology 87, 691–698.
Leritz, E.C., Salat, D.H., Williams, V.J., Schnyer, D.M., Rudolph, J.L., Lipsitz, L., Fischl, B., McGlinchey, R.E., Milberg, W.P., 2011. Thickness of the human cerebral cortex is associated with metrics of cerebrovascular health in a normative sample of community dwelling older adults. Neuroimage 54, 2659–2671.
Lucas, J.A., Ivnik, R.J., Smith, G.E., Bohac, D.L., Tangalos, E.G., Graff-Radford, N.R., Petersen, R.C., 1998. Mayo's older Americans normative studies: category fluency norms. J. Clin. Exp. Neuropsychol. 20, 194–200.
Machulda, M.M., Pankratz, V.S., Christianson, T.J., Ivnik, R.J., Mielke, M.M., Roberts, R.O., Knopman, D.S., Boeve, B.F., Petersen, R.C., 2013. Practice effects and longitudinal cognitive change in normal aging vs. incident mild cognitive impairment and dementia in the Mayo Clinic Study of Aging. Clin. Neuropsychol. 27, 1247–1264.
Mattsson, N., Insel, P.S., Aisen, P.S., Jagust, W., Mackin, S., Weiner, M., 2015. Brain structure and function as mediators of the effects of amyloid on memory. Neurology 84, 1136–1144.
Mormino, E.C., Betensky, R.A., Hedden, T., Schultz, A.P., Amariglio, R.E., Rentz, D.M., Johnson, K.A., Sperling, R.A., 2014. Synergistic effect of beta-amyloid and neurodegeneration on cognitive decline in clinically normal individuals. JAMA Neurol. 71, 1379–1385.
Mormino, E.C., Brandel, M.G., Madison, C.M., Rabinovici, G.D., Marks, S., Baker, S.L., Jagust, W.J., 2012. Not quite PIB-positive, not quite PIB-negative: Slight PIB elevations in elderly normal control subjects are biologically relevant. Neuroimage 59, 1152–1160.
Murray, M.E., Lowe, V.J., Graff-Radford, N.R., Liesinger, A.M., Cannon, A., Przybelski, S.A., Rawal, B., Parisi, J.E., Petersen, R.C., Kantarci, K., Ross, O.A., Duara, R., Knopman, D.S., Jack Jr., C.R., Dickson, D.W., 2015. Clinicopathologic and 11C-Pittsburgh compound B implications of Thal amyloid phase across the Alzheimer's disease spectrum. Brain 138, 1370–1381.
Musiek, E.S., Holtzman, D.M., 2015. Three dimensions of the amyloid hypothesis: time, space and 'wingmen'. Nat. Neurosci. 18, 800–806.
Nelson, P.T., Head, E., Schmitt, F.A., Davis, P.R., Neltner, J.H., Jicha, G.A., Abner, E.L., Smith, C.D., Van Eldik, L.J., Kryscio, R.J., Scheff, S.W., 2011. Alzheimer's disease is not "brain aging": neuropathological, genetic, and epidemiological human studies. Acta Neuropathol. 121, 571–587.
Ossenkoppele, R., Schonhaut, D.R., Scholl, M., Lockhart, S.N., Ayakta, N., Baker, S.L., O'Neil, J.P., Janabi, M., Lazaris, A., Cantwell, A., Vogel, J., Santos, M., Miller, Z.A., Bettcher, B.M., Vossel, K.A., Kramer, J.H., Gorno-Tempini, M.L., Miller, B.L., Jagust, W.J., Rabinovici, G.D., 2016. Tau PET patterns mirror clinical and neuroanatomical variability in Alzheimer's disease. Brain 139, 1551–1567.
Petersen, R.C., 2004. Mild cognitive impairment as a diagnostic entity. J. Intern. Med. 256, 183–194.
Petersen, R.C., Roberts, R.O., Knopman, D.S., Geda, Y.E., Cha, R.C., Pankratz, V.S., Boeve, B.F., Tangalos, E.G., Ivnik, R.J., Rocca, W.A., 2010. Prevalence of mild cognitive impairment is higher in men than in women. The Mayo Clinic Study of Aging. Neurology 75, 889–897.
Petersen, R.C., Wiste, H.J., Weigand, S.D., Rocca, W.A., Roberts, R.O., Mielke, M.M., Lowe, V.J., Knopman, D.S., Pankratz, V.S., Machulda, M.M., Geda, Y.E., Jack Jr., C.R., 2015. Association of elevated amyloid levels with cognition and biomarkers in cognitively normal people from the community. JAMA Neurol. 73, 85–92.
Raz, N., Lindenberger, U., Rodrigue, K.M., Kennedy, K.M., Head, D., Williamson, A., Dahle, C., Gerstorf, D., Acker, J.D., 2005. Regional brain changes in aging healthy adults: general trends, individual differences and modifiers. Cereb. Cortex 15, 1676–1689.
Reitan, R., 1958. Validity of the Trail-making test as an indication of organic brain damage. Percept. Mot. Skills 8, 271–276.
Roberts, R.O., Geda, Y.E., Knopman, D., Cha, R., Pankratz, V.S., Boeve, B., Ivnik, R., Tangalos, E., Petersen, R.C., Rocca, W.A., 2008. The Mayo Clinic Study of Aging: design and sampling, participation, baseline measures and sample characteristics. Neuroepidemiology 30, 58–69.
Roberts, R.O., Geda, Y.E., Knopman, D.S., Cha, R.H., Pankratz, V.S., Boeve, B.F., Tangalos, E.G., Ivnik, R.J., Rocca, W.A., Petersen, R.C., 2012. The incidence of MCI differs by subtype and is higher in men: the Mayo Clinic Study of Aging. Neurology 78, 342–351.
Roberts, R.O., Knopman, D.S., Mielke, M.M., Cha, R.H., Pankratz, V.S., Christianson, T.J., Geda, Y.E., Boeve, B.F., Ivnik, R.J., Tangalos, E.G., Rocca, W.A., Petersen, R.C., 2014. Higher risk of progression to dementia in mild cognitive impairment cases who revert to normal. Neurology 82, 317–325.
Rowe, C.C., Ellis, K.A., Rimajova, M., Bourgeat, P., Pike, K.E., Jones, G., Fripp, J., Tochon-Danguy, H., Morandeau, L., O'Keefe, G., Price, R., Raniga, P., Robins, P., Acosta, O., Lenzo, N., Szoeke, C., Salvado, O., Head, R., Martins, R., Masters, C.L., Ames, D., Villemagne, V.L., 2010. Amyloid imaging results from the Australian Imaging, Biomarkers and Lifestyle (AIBL) study of aging. Neurobiol. Aging 31, 1275–1283.
Sabayan, B., van Buchem, M.A., Sigurdsson, S., Zhang, Q., Harris, T.B., Gudnason, V., Arai, A.E., Launer, L.J., 2015. Cardiac hemodynamics are linked with structural and functional features of brain aging: the age, gene/environment susceptibility (AGES)-Reykjavik Study. J. Am. Heart Assoc. 4, e001294.
Sabuncu, M.R., Desikan, R.S., Sepulcre, J., Yeo, B.T., Liu, H., Schmansky, N.J., Reuter, M., Weiner, M.W., Buckner, R.L., Sperling, R.A., Fischl, B., 2011. The dynamics of cortical and hippocampal atrophy in Alzheimer disease. Arch. Neurol. 68, 1040–1048.
Salat, D.H., Buckner, R.L., Snyder, A.Z., Greve, D.N., Desikan, R.S., Busa, E., Morris, J.C., Dale, A.M., Fischl, B., 2004. Thinning of the cerebral cortex in aging. Cereb. Cortex 14, 721–730.
Savva, G.M., Wharton, S.B., Ince, P.G., Forster, G., Matthews, F.E., Brayne, C., 2009. Age, neuropathology, and dementia. N. Engl. J. Med. 360, 2302–2309.

Scholl, M., Lockhart, S.N., Schonhaut, D.R., O'Neil, J.P., Janabi, M., Ossenkoppele, R., Baker, S.L., Vogel, J.W., Faria, J., Schwimmer, H.D., Rabinovici, G.D., Jagust, W.J., 2016. PET imaging of tau deposition in the aging human brain. Neuron 89, 971–982.

Schwarz, A.J., Yu, P., Miller, B.B., Shcherbinin, S., Dickson, J., Navitsky, M., Joshi, A.D., Devous Sr., M.D., Mintun, M.S., 2016a. Regional profiles of the candidate tau PET ligand 18F-AV-1451 recapitulate key features of Braak histopathological stages. Brain 139, 1539–1550.

Schwarz, C.G., Gunter, J.L., Wiste, H.J., Przybelski, S.A., Weigand, S.D., Ward, C.P., Senjem, M.L., Vemuri, P., Murray, M.E., Dickson, D.W., Parisi, J.E., Kantarci, K., Weiner, M.W., Petersen, R.C., Jack, C.R.J., 2016b. A large scale comparison of cortical thickness and volume methods for measuring Alzheimer's disease severity. Neuroimage Clin. 11, 802–812.

Toledo, J.B., Weiner, M.W., Wolk, D.A., Da, X., Chen, K., Arnold, S.E., Jagust, W., Jack, C., Reiman, E.M., Davatzikos, C., Shaw, L.M., Trojanowski, J.Q., 2014. Neuronal injury biomarkers and prognosis in ADNI subjects with normal cognition. Acta Neuropathol. Commun. 2, 26.

Tzourio-Mazoyer, N., Landeau, B., Papathanassiou, D., Crivello, F., Etard, O., Delcroix, N., Mazoyer, B., Joliot, M., 2002. Automated anatomical labeling of activations in SPM using a macroscopic anatomical parcellation of the MNI MRI single-subject brain. Neuroimage 15, 273–289.

Vemuri, P., Lesnick, T.G., Przybelski, S.A., Knopman, D.S., Lowe, V.J., Graff-Radford, J., Roberts, R.O., Mielke, M.M., Machulda, M.M., Petersen, R.C., Jack Jr., C.R., 2017a. Age, vascular health, and Alzheimer disease biomarkers in an elderly sample. Ann. Neurol. 82, 706–718.

Vemuri, P., Lowe, V.J., Knopman, D.S., Senjem, M.L., Kemp, B.J., Schwarz, C.G., Przybelski, S.A., Machulda, M.M., Petersen, R.C., Jack Jr., C.R., 2017b. Tau-PET uptake: regional variation in average SUVR and impact of amyloid deposition. Alzheimers Dement. (Amst) 6, 21–30.

Vemuri, P., Wiste, H.J., Weigand, S.D., Shaw, L.M., Trojanowski, J.Q., Weiner, M.W., Knopman, D.S., Petersen, R.C., Jack Jr., C.R., 2009. MRI and CSF biomarkers in normal, MCI, and AD subjects: predicting future clinical change. Neurology 73, 294–301.

Villemagne, V.L., Burnham, S., Bourgeat, P., Brown, B., Ellis, K.A., Salvado, O., Szoeke, C., Macaulay, S.L., Martins, R., Maruff, P., Ames, D., Rowe, C.C., Masters, C.L., 2013. Amyloid beta deposition, neurodegeneration, and cognitive decline in sporadic Alzheimer's disease: a prospective cohort study. Lancet Neurol. 12, 357–367.

Villemagne, V.L., Pike, K.E., Chetelat, G., Ellis, K.A., Mulligan, R.S., Bourgeat, P., Ackermann, U., Jones, G., Szoeke, C., Salvado, O., Martins, R., O'Keefe, G., Mathis, C.A., Klunk, W.E., Ames, D., Masters, C.L., Rowe, C.C., 2011. Longitudinal assessment of Abeta and cognition in aging and Alzheimer disease. Ann. Neurol. 69, 181–192.

Villeneuve, S., Rabinovici, G.D., Cohn-Sheehy, B.I., Madison, C., Ayakta, N., Ghosh, P.M., La Joie, R., Arthur-Bentil, S.K., Vogel, J.W., Marks, S.M., Lehmann, M., Rosen, H.J., Reed, B., Olichney, J., Boxer, A.L., Miller, B.L., Borys, E., Jin, L.W., Huang, E.J., Grinberg, L.T., DeCarli, C., Seeley, W.W., Jagust, W., 2015. Existing Pittsburgh Compound-B positron emission tomography thresholds are too high: statistical and pathological evaluation. Brain 138, 2020–2033.

Villeneuve, S., Reed, B.R., Wirth, M., Haase, C.M., Madison, C.M., Ayakta, N., Mack, W., Mungas, D., Chui, H.C., DeCarli, C., Weiner, M.W., Jagust, W.J., 2014. Cortical thickness mediates the effect of beta-amyloid on episodic memory. Neurology 82, 761–767.

Wechsler, D., 1981. Wechsler Adult Intelligence Scale-Revised. The Psychological Corporation, New York.

Wechsler, D.A., 1987. Wechsler Memory Scale-Revised. Psychological Corporation, New York.

Weston, P.S., Nicholas, J.M., Lehmann, M., Ryan, N.S., Liang, Y., Macpherson, K., Modat, M., Rossor, M.N., Schott, J.M., Ourselin, S., Fox, N.C., 2016. Presymptomatic cortical thinning in familial Alzheimer disease: a longitudinal MRI study. Neurology 87, 2050–2057.

Whitwell, J.L., Tosakulwong, N., Weigand, S.D., Senjem, M.L., Lowe, V.J., Gunter, J.L., Boeve, B.F., Knopman, D.S., Dickerson, B.C., Petersen, R.C., Jack Jr., C.R., 2013. Does amyloid deposition produce a specific atrophic signature in cognitively normal subjects? Neuroimage Clin. 2, 249–257.

Wirth, M., Madison, C.M., Rabinovici, G.D., Oh, H., Landau, S.M., Jagust, W.J., 2013a. Alzheimer's disease neurodegenerative biomarkers are associated with decreased cognitive function but not beta-amyloid in cognitively normal older individuals. J. Neurosci. 33, 5553–5563.

Wirth, M., Oh, H., Mormino, E.C., Markley, C., Landau, S.M., Jagust, W.J., 2013b. The effect of amyloid beta on cognitive decline is modulated by neural integrity in cognitively normal elderly. Alzheimers Dement. 9, 687–698.

Xia, C., Makaretz, S.J., Caso, C., McGinnis, S., Gomperts, S.N., Sepulcre, J., Gomez-Isla, T., Hyman, B.T., Schultz, A., Vasdev, N., Johnson, K.A., Dickerson, B.C., 2017. Association of in vivo [18F]AV-1451 tau PET imaging results with cortical atrophy and symptoms in typical and atypical Alzheimer disease. JAMA Neurol. 74, 427–436.